

Science

 AAAS

**CRISPR Provides Acquired Resistance Against
Viruses in Prokaryotes**

Rodolphe Barrangou, *et al.*

Science **315**, 1709 (2007);

DOI: 10.1126/science.1138140

***The following resources related to this article are available online at
www.sciencemag.org (this information is current as of November 13, 2007):***

Updated information and services, including high-resolution figures, can be found in the online version of this article at:

<http://www.sciencemag.org/cgi/content/full/315/5819/1709>

Supporting Online Material can be found at:

<http://www.sciencemag.org/cgi/content/full/315/5819/1709/DC1>

A list of selected additional articles on the Science Web sites **related to this article** can be found at:

<http://www.sciencemag.org/cgi/content/full/315/5819/1709#related-content>

This article **cites 20 articles**, 9 of which can be accessed for free:

<http://www.sciencemag.org/cgi/content/full/315/5819/1709#otherarticles>

This article has been **cited by** 10 article(s) on the ISI Web of Science.

This article has been **cited by** 3 articles hosted by HighWire Press; see:

<http://www.sciencemag.org/cgi/content/full/315/5819/1709#otherarticles>

This article appears in the following **subject collections**:

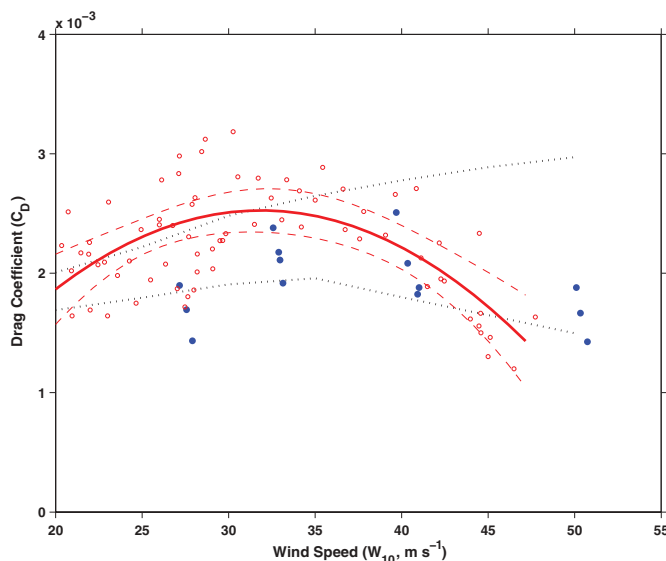
Microbiology

<http://www.sciencemag.org/cgi/collection/microbio>

Information about obtaining **reprints** of this article or about obtaining **permission to reproduce this article** in whole or in part can be found at:

<http://www.sciencemag.org/about/permissions.dtl>

Fig. 3. Drag coefficient as a function of wind speed. C_D is shown for an observation-based resistance coefficient, $r = 0.02 \text{ cm s}^{-1}$. The red open circles are the evaluated C_D from the current and wind observations, the solid red line is a fitted quadratic curve to the C_D estimates, and the red dashed lines are the 95% confidence limits for this quadratic curve. The black dotted lines represent the window for C_D reported in (6), whereas the blue dots represent C_D reported in (4).



speeds below 30 m s^{-1} , are somewhat noisy as a result of measurement uncertainty and the need to calculate a velocity derivative, which tends to enhance noise. However, they consistently show a decreasing trend of C_D for wind speeds greater than 32 m s^{-1} , the lower threshold for a category 1 hurricane on the Saffir-Simpson Scale. It is also apparent that the C_D values are weakly dependent on the choice of the resistance coefficient and are larger for increasing values of r . The drag coefficient estimates evaluated for $r = 0.1 \text{ cm s}^{-1}$ are, on average, 20% greater than those calculated for $r = 0.001 \text{ cm s}^{-1}$ from Eq. 3.

To produce the best representation of C_D for each r , a second-order curve (a function of the wind speed) was fitted by a least-squares technique to all estimated values of C_D . The curves are displayed in Figs. 2 and 3. Additionally, the 95% confidence limits for the fitted curve are shown in Fig. 3. The pattern of the relationship between C_D and the wind speed is robust, but the curve coefficients are determined by the value chosen for r in Eq. 3. However, all curves clearly show an initial increase of the drag coefficient and monotonic decrease as found by recent studies (3–8) after reaching a maximum value at $\sim 32 \text{ m s}^{-1}$. Some of these studies (3, 19) imply that the decreasing drag at high winds seems to be related to the spray, foam, and bubbles from breaking waves that reduce the drag and allow the hurricane to slip over the sea.

With the nearly full water-column ocean current measurements, the only unknown term left in the simplified equation of motion is the wind stress. Thus, the behavior of the drag coefficient (C_D) can easily be estimated for a range of strong winds. Despite the fact that the drag coefficient is evaluated differently here, estimates of C_D determined “bottom-up” reasonably replicate the values determined “top-down” in recent studies (3–7). Results from our research show that C_D peaks at a wind speed near 32 m s^{-1} and

then steadily decreases as the wind speed continues to rise. Our values for C_D are in a range of C_D values found using meteorological observations (4) for wind speeds greater than 32 m s^{-1} but are higher for lower wind speeds. These differences may be attributed to uncertainties in the wind measurements and the applicability of the simplified ocean dynamics at the lower wind speeds.

References and Notes

1. K. Emanuel, *Nature* **436**, 686 (2005).
2. S. E. Larsen *et al.*, in *Wind Stress Over the Ocean*, I. S. F. Jones, Y. Toba, Eds. (Cambridge Univ. Press, New York, 2001), chap. 7.
3. M. A. Donelan *et al.*, *Geophys. Res. Lett.* **31**, L18306 10.1029/2004GL019460 (2004).

4. M. D. Powell, P. J. Vickery, T. A. Reinhold, *Nature* **422**, 279 (2003).
5. E. D. Fernandez *et al.*, *J. Geophys. Res.* **111**, C08013 10.1029/2005JG003048 (2006).
6. I. J. Moon, I. Ginis, T. Hara, *J. Atmos. Sci.* **61**, 2334 (2004).
7. J. A. T. Bye, A. D. Jenkins, *J. Geophys. Res.* **111**, C03024 10.1029/2005JG003114 (2006).
8. K. Emanuel, *J. Atmos. Sci.* **60**, 1420 (2003).
9. D. A. Mitchell, W. J. Teague, E. Jarosz, D. W. Wang, *Geophys. Res. Lett.* **32**, L11610 10.1029/2005GL023014 (2005).
10. D. W. Wang, D. A. Mitchell, W. J. Teague, E. Jarosz, M. S. Hulbert, *Science* **309**, 896 (2005).
11. W. J. Teague, E. Jarosz, D. W. Wang, D. A. Mitchell, *J. Phys. Oceanogr.*, in press.
12. W. J. Teague, E. Jarosz, M. R. Carnes, D. A. Mitchell, P. J. Hogan, *Cont. Shelf Res.* **26**, 2559 (2006).
13. J. F. Price, T. B. Sanford, G. Z. Forristall, *J. Phys. Oceanogr.* **24**, 233 (1994).
14. Materials and methods are available as supporting material on Science Online.
15. G. T. Mitchum, W. Sturges, *J. Phys. Oceanogr.* **12**, 1310 (1982).
16. S. T. Lentz, *J. Phys. Oceanogr.* **24**, 2461 (1994).
17. S. J. Lentz, *J. Phys. Oceanogr.* **31**, 2749 (2001).
18. J. M. Pringle, *J. Phys. Oceanogr.* **32**, 3101 (2002).
19. E. L. Andreas, *J. Phys. Oceanogr.* **34**, 1429 (2004).
20. We thank M. S. Hulbert, A. J. Quaid, and W. A. Goode for mooring support. We also thank the crews of the research vessels Seward Johnson I and II. This work was supported by the Office of Naval Research as a part of the Naval Research Laboratory’s basic research project “Slope to Shelf Energetics and Exchange Dynamics (SEED)” under program element 0601153N, through the Minerals Management Service Environmental Studies Program Technology, and by the Minerals Management Service Technology Assessment and Research Program on Hurricane Ivan.

Supporting Online Material

www.sciencemag.org/cgi/content/full/315/5819/1707/DC1
SOM Text

Fig. S1
References

18 October 2006; accepted 14 February 2007
10.1126/science.1136466

CRISPR Provides Acquired Resistance Against Viruses in Prokaryotes

Rodolphe Barrangou,¹ Christophe Fremaux,² H el ene Deveau,³ Melissa Richards,¹ Patrick Boyaval,² Sylvain Moineau,³ Dennis A. Romero,¹ Philippe Horvath^{2*}

Clustered regularly interspaced short palindromic repeats (CRISPR) are a distinctive feature of the genomes of most Bacteria and Archaea and are thought to be involved in resistance to bacteriophages. We found that, after viral challenge, bacteria integrated new spacers derived from phage genomic sequences. Removal or addition of particular spacers modified the phage-resistance phenotype of the cell. Thus, CRISPR, together with associated *cas* genes, provided resistance against phages, and resistance specificity is determined by spacer-phage sequence similarity.

Bacteriophages are arguably the most abundant biological entity on the planet (1). Their ubiquitous distribution and abundance have an important impact on microbial ecology and the evolution of bacterial genomes (2). Consequently, bacteria have developed a variety of natural defense mechanisms that target diverse steps of the phage life cycle, notably blocking adsorption, preventing DNA

injection, restricting the incoming DNA, and abortive infection systems. These antiviral barriers can also be engineered and manipulated to better control phage populations (2, 3).

Numerous bacteria have been selected by humans and used extensively for fermentation and biotechnology processes. Unfortunately, domesticated bacteria used in industrial applications are often susceptible to phage attack, including

genera and species widely used as dairy cultures (4). Accordingly, the industry has devised various strategies to combat phage based on strain diversity, bacteriophage-insensitive mutants, and plasmids bearing phage-resistance mechanisms.

Streptococcus thermophilus is a low G+C Gram-positive bacterium and a key species exploited in the formulation of dairy culture systems for the production of yogurt and cheese. Comparative genomics analyses of closely related *S. thermophilus* strains have previously revealed that genetic polymorphism primarily occurs at hypervariable loci, such as the *eps* and *rps* operons, as well as two clustered regularly interspaced short palindromic repeats (CRISPR) loci (5–7). CRISPR loci typically consist of several noncontiguous direct repeats separated by stretches of variable sequences called spacers and are oftentimes adjacent to *cas* genes (CRISPR-associated). Although the function of CRISPR loci has not been established biologically, in silico analyses of the spacers have revealed sequence homology with foreign elements, including bacteriophage and plasmid sequences (7–9). Based exclusively on in silico analyses, several hypotheses have been put forward proposing roles for CRISPR and *cas* genes, which include providing immunity against foreign genetic elements via a mechanism based on RNA interference (10).

We analyzed the CRISPR sequences of various *S. thermophilus* strains, including closely related industrial strains and phage-resistant variants (fig. S1). Differences in the number and type of spacers were observed primarily at the CRISPR1 locus. Notably, phage sensitivity appeared to be correlated with CRISPR1 spacer content. Specifically, spacer content was nearly identical between parental strains and phage-resistant derivatives, except for additional spacers present in the latter. These findings therefore suggest a potential relation between the presence of additional spacers and the differences observed in the phage sensitivity of a given strain. This observation prompted us to investigate the origin and function of additional spacers present in phage-resistant mutants.

First, we tested the hypothesis that CRISPR loci are altered during the natural generation of phage-resistant mutants. A phage-host model system was selected, consisting of a phage-sensitive wild-type *S. thermophilus* strain widely used in the dairy industry, DGCC7710 [wild type (WT)] and two distinct but closely related virulent bacteriophages isolated from industrial yogurt samples, phage 858 and phage 2972 (11).

Nine phage-resistant mutants were generated independently by challenging the WT strain with phage 858, phage 2972, or simultaneously with both (12), and their CRISPR loci were analyzed. Differences were consistently observed at the CRISPR1 locus, where 1 to 4 additional spacers were inserted next to the 32 spacers present in the WT strain (Fig. 1). The addition of new spacers in response to phage infection seemed to be polarized toward one end of the CRISPR1 locus. This is consistent with previous observations of spacer hypervariability at the leader end of the CRISPR locus in various strains (9, 13). Sequence analysis of the additional spacers inserted

in the CRISPR1 locus of the various phage-resistant mutants revealed similarity to sequences found within the genomes of the phages used in the challenge (Fig. 2 and fig. S2). Interestingly, similarities were observed throughout the phage genomes, in most functional modules, both on the coding and noncoding strands. No particular sequence, gene, or functional group seemed to be targeted specifically. These results reveal that, on becoming resistant to bacteriophages, the CRISPR1 locus was modified by the integration of novel spacers, apparently derived from phage DNA.

Surprisingly, we observed that some strains were resistant to both phages, whereas others

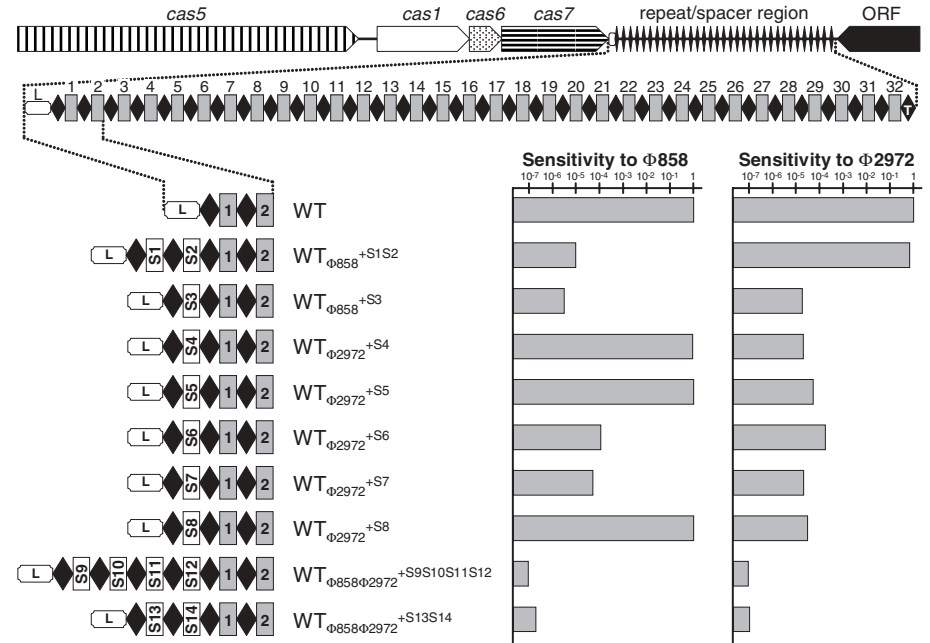


Fig. 1. *Streptococcus thermophilus* CRISPR1 locus overview, newly acquired spacers in phage-resistant mutants, and corresponding phage sensitivity. The CRISPR1 locus of DGCC7710 (WT) is at the top. The repeat-spacer region of WT is in the middle: repeats (black diamonds), spacers (numbered gray boxes), leader (L, white box), and terminal repeat (T, black diamond). (Bottom left) The spacer content on the leader side of the locus in phage-resistant mutants is detailed, with newly acquired spacers (white boxes, S1 to S14). (Bottom right) The sensitivity of each strain to phages 858 and 2972 is represented as a histogram of the efficiency of plaquing (EOP), which is the plaque count ratio of a mutant strain to that of the wild-type.

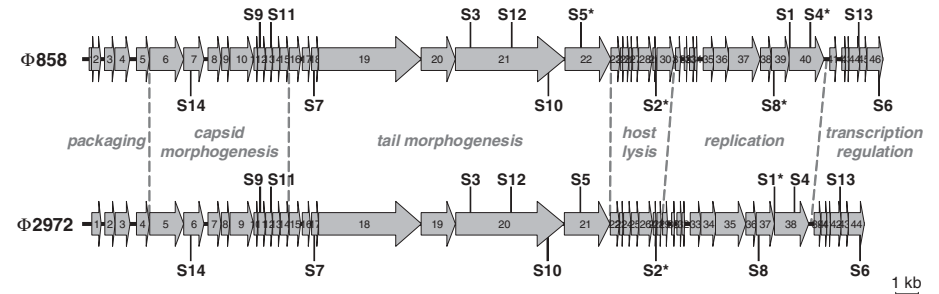


Fig. 2. *S. thermophilus* phage genome maps with the position of sequences similar to the acquired CRISPR1 spacers of the phage-resistant mutants. Spacers shown above and below the genome maps indicate that the spacer matches a sequence on the (+) and on the (–) strand, respectively. An asterisk indicates the existence of a SNP between the spacer sequence and that of the phage genome (fig. S1). The genome sequences of phage 2972 (accession number AY699705) and phage 858 are 93% identical.

¹Danisco USA Inc., 3329 Agriculture Drive, Madison, WI 53716, USA. ²Danisco France SAS, Boîte Postale 10, F-86220 Dangé-Saint-Romain, France. ³Département de Biochimie et de Microbiologie, Faculté des Sciences et de Génie, Groupe de Recherche en Ecologie Buccale, Faculté de Médecine Dentaire, Félix d'Hérelle Reference Center for Bacterial Viruses, Université Laval, G1K 7P4 Québec, Canada.

*To whom correspondence should be addressed. E-mail: philippe.horvath@danisco.com

were resistant only to the phage used in the challenge (Fig. 1). The phage-resistance profile seemed correlated to the spacer content, such that strains with spacers showing 100% identity to sequences conserved in both phages were resistant to both phages, such as spacers S3, S6, and S7. In contrast, when nucleotide polymorphisms were observed between the spacer and the phage sequence [from 1 to 15 single-nucleotide polymorphisms (SNPs) over 29 or 30 nucleotides], the spacer did not seem to provide resistance, such as spacers S1, S2, S4, S5, and S8 (Fig. 1 and fig. S2). In addition, when several spacers were inserted (S9 to S14), phage resistance levels were higher. These findings indicate that the CRISPR1 locus is subject to dynamic and rapid evolutionary changes driven by phage exposure. Altogether, these results reveal that CRISPR loci can indeed be altered during the generation of phage-resistant mutants and also establish a link between CRISPR content and phage sensitivity. These findings suggest that the presence of a CRISPR spacer identical to a phage sequence provides resistance against phages containing this particular sequence.

To determine whether CRISPR spacer content defines phage resistance, we altered the CRISPR1 locus by adding and deleting spacers (12) and tested subsequent strain sensitivity to phages. All constructs were generated and integrated into the *S. thermophilus* chromosome with the system developed by Russell and Klaenhammer (14). We removed the spacers and repeats in the CRISPR1 locus of strain $WT_{\Phi 858}^{+S1S2}$ and replaced them with a single repeat without any spacer (12). The resulting strain $WT_{\Phi 858}^{+S1S2}\Delta CRISPR1$ was sensitive to phage 858, which indicated that the phage resistance of the original phage-resistant mutant ($WT_{\Phi 858}^{+S1S2}$) was probably linked to the presence of S1 and S2 (Fig. 3).

Further, to address the critical question of whether adding spacers provides novel phage resistance, we replaced the CRISPR1 locus of strain $WT_{\Phi 2972}^{+S4}$ with a version containing only spacers S1 and S2 (12) and tested whether the phage sensitivity was affected. Remarkably, the resulting strain $WT_{\Phi 2972}^{+S4}::pS1S2$ gained resistance to phage 858, which suggested that these two spacers have the ability to provide phage resistance de novo (Fig. 3). Altogether,

these observed modifications establish the link between the CRISPR spacer content and phage resistance.

In the process of generating strain $WT_{\Phi 858}^{+S1S2}\Delta CRISPR1$, we created $WT_{\Phi 858}^{+S1S2}::pR$, a variant that contains the integration vector with a single repeat inserted between the *cas* genes and the native CRISPR1 locus (Fig. 3). Unexpectedly, strain $WT_{\Phi 858}^{+S1S2}::pR$ was sensitive to phage 858, although spacers S1 and S2 remained on the chromosome (Fig. 3). Similarly, the $WT_{\Phi 2972}^{+S4}::pS1S2$ construct lost the resistance to phage 2972, although spacer S4 is present in the chromosome (Fig. 3). These results indicated that spacers alone did not provide resistance, and perhaps, that they have to be in a particular genetic context to be effective.

Although initial work suggested involvement in DNA repair (15), the current hypothesis is that *cas* genes (5, 16) are involved in CRISPR-mediated immunity (10). Consequently, we inactivated two *cas* genes in strain $WT_{\Phi 858}^{+S1S2}$ (12): *cas5* (COG3513) and *cas7*, which are equivalent to *str0657/stu0657* and *str0660/stu0660*, respectively (6, 7). The *cas5* inactivation resulted in loss of the phage resistance (Fig. 3), and perhaps Cas5 acts as a nuclease, because it contains an HNH-type nuclease motif. In contrast, inactivating *cas7* did not alter the resistance to phage 858 (Fig. 3). Interestingly, we were repeatedly unable to generate CRISPR1 phage-resistant mutants from the *cas7* knockout, perhaps because Cas7 is involved in the synthesis and/or insertion of new spacers and additional repeats.

When we tested the sensitivity of the phage-resistant mutants, we found that plaque formation was dramatically reduced, but that a relatively small population of bacteriophage retained the ability to infect the mutants. We further analyzed phage variants derived from phage 858 that retained the ability to infect $WT_{\Phi 858}^{+S1S2}$. In particular, we investigated the sequence of the genome region corresponding to additional spacers S1 and S2 in two virulent phage variants. In both cases, the genome sequence of the phage variant had mutated, and two distinct SNPs were identified in the sequence corresponding to spacer S1 (fig. S3).

Overall, prokaryotes appear to have evolved a nucleic acid–based “immunity” system whereby specificity is dictated by the CRISPR spacer content, while the resistance is provided by the Cas enzymatic machinery. Additionally, we speculate that some of the *cas* genes not directly providing resistance are actually involved in the insertion of additional CRISPR spacers and repeats, as part of an adaptive “immune” response. Further studies are desired to better characterize the mechanism of action and to identify the specific function of the various *cas* genes. This nucleic acid–based system contrasts with amino acid–based counterparts in eukaryotes through which adaptive immunity is not inheritable.

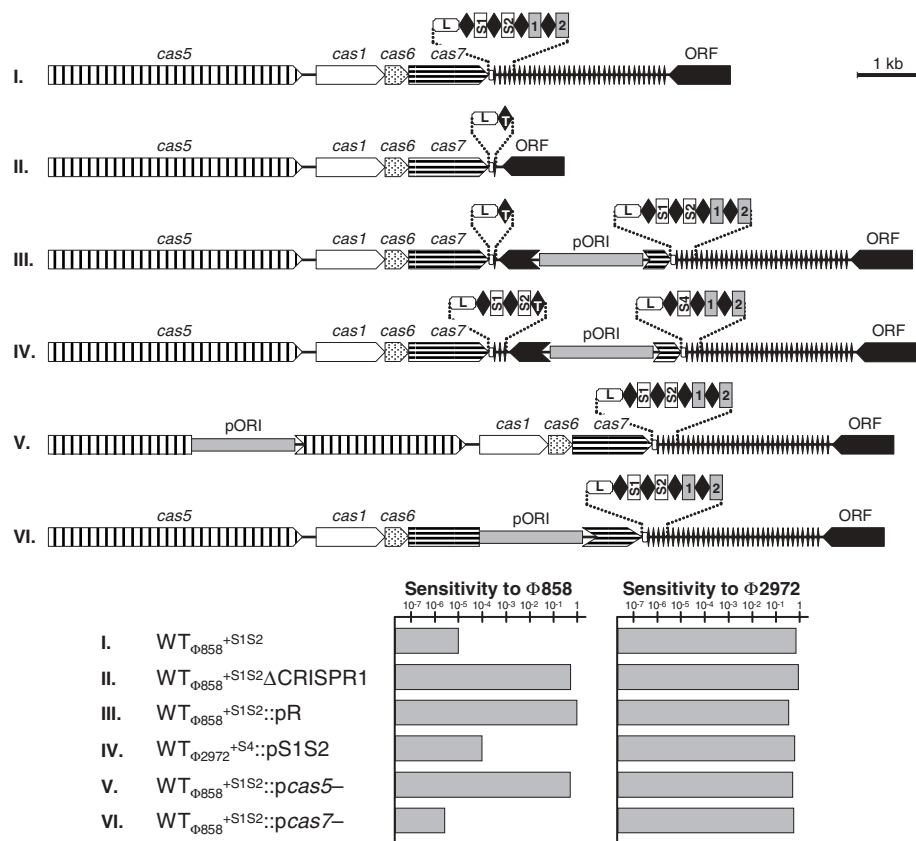


Fig. 3. CRISPR spacer engineering, *cas* gene inactivation, and corresponding phage sensitivity. I, mutant $WT_{\Phi 858}^{+S1S2}$; II, mutant $WT_{\Phi 858}^{+S1S2}\Delta CRISPR1$ in which CRISPR1 was deleted; III, mutant $WT_{\Phi 858}^{+S1S2}::pR$ in which CRISPR1 was displaced and replaced with a unique repeat; IV, $WT_{\Phi 2972}^{+S4}::pS1S2$, mutant of strain $WT_{\Phi 2972}^{+S4}$ in which CRISPR1 was displaced and replaced with a version containing S1 and S2; V, $WT_{\Phi 858}^{+S1S2}::pcas5-$ with *cas5* inactivated; VI, $WT_{\Phi 858}^{+S1S2}::pcas7-$ with *cas7* inactivated. pORI indicates the integrated plasmid (12). The phage sensitivity of each strain to phages 858 and 2972 is represented at the bottom as a histogram of the efficiency of plating (EOP).

The inheritable nature of CRISPR spacers supports the use of CRISPR loci as targets for evolutionary, typing, and comparative genomic studies (9, 17–19). Because this system is reactive to the phage environment, it likely plays a significant role in prokaryotic evolution and ecology and provides a historical perspective of phage exposure, as well as a predictive tool for phage sensitivity. The CRISPR-cas system may accordingly be exploited as a virus defense mechanism and also potentially used to reduce the dissemination of mobile genetic elements and the acquisition of undesirable traits such as antibiotic resistance genes and virulence markers. From a phage evolution perspective, the integrated phage sequences within CRISPR loci may also provide additional anchor points to facilitate recombination during subsequent phage infections, thus increasing the gene pool to which phages have access (20). Because CRISPR loci are found in the majority of bacterial genera and are ubiquitous in Archaea (5, 13, 21), their study will provide new insights into the relation and codirected evolution between prokaryotes and their predators.

References and Notes

- M. Breitbart, F. Rohwer, *Trends Microbiol.* **13**, 278 (2005).
- S. Chibani-Chennoufi, A. Bruttin, M.-L. Dillmann, H. Brüssow, *J. Bacteriol.* **186**, 3677 (2004).
- J. M. Sturino, T. R. Klaenhammer, *Nat. Rev. Microbiol.* **4**, 395 (2006).
- H. Brüssow, *Annu. Rev. Microbiol.* **55**, 283 (2001).
- R. Jansen, J. D. A. van Embden, W. Gaastra, L. M. Schouls, *Mol. Microbiol.* **43**, 1565 (2002).
- A. Bolotin *et al.*, *Nat. Biotechnol.* **22**, 1554 (2004).
- A. Bolotin, B. Quinquis, A. Sorokin, S. D. Ehrlich, *Microbiology* **151**, 2551 (2005).
- F. J. M. Mojica, C. Díez-Villaseñor, J. García-Martínez, E. Soria, *J. Mol. Evol.* **60**, 174 (2005).
- C. Pourcel, G. Salvignol, G. Vergnaud, *Microbiology* **151**, 653 (2005).
- K. S. Makarova, N. V. Grishin, S. A. Shabalina, Y. I. Wolf, E. V. Koonin, *Biol. Direct* **1**, 7 (2006).
- C. Lévesque *et al.*, *Appl. Environ. Microbiol.* **71**, 4057 (2005).
- Information on materials and methods for the generation of phage-resistant mutants, engineering of CRISPR spacers (Figs. S4 and S5), and inactivation of *cas* genes is available on Science Online.
- R. K. Lillestøl, P. Redder, R. A. Garrett, K. Brügger, *Archaea* **2**, 59 (2006).
- W. M. Russell, T. R. Klaenhammer, *Appl. Environ. Microbiol.* **67**, 4361 (2001).
- K. S. Makarova, L. Aravind, N. V. Grishin, I. B. Rogozin, E. V. Koonin, *Nucleic Acids Res.* **30**, 482 (2002).
- D. H. Haft, J. Selengut, E. F. Mongodin, K. E. Nelson, *PLoS Comput. Biol.* **1**, e60 (2005).
- P. M. A. Groenen, A. E. Bunschoten, D. van Soolingen, J. D. A. van Embden, *Mol. Microbiol.* **10**, 1057 (1993).
- E. F. Mongodin *et al.*, *J. Bacteriol.* **187**, 4935 (2005).
- R. T. DeBoy, E. F. Mongodin, J. B. Emerson, K. E. Nelson, *J. Bacteriol.* **188**, 2364 (2006).
- R. W. Hendrix *et al.*, *Proc. Natl. Acad. Sci. U.S.A.* **96**, 2192 (1999).
- J. S. Godde, A. Bickerton, *J. Mol. Evol.* **62**, 718 (2006).
- We thank L. Bayer, C. Vos, and A.-C. Couëté-Monvoisin of Danisco Innovation, as well as J. Labonté and D. Tremblay of Université Laval for technical support, and E. Bech Hansen for discussions and critical review of the manuscript. Also, we thank T. R. Klaenhammer for providing the integration system. This work was supported by funding from Danisco A/S. Also, S. M. would like to acknowledge support from the Natural Sciences and Engineering Research Council of Canada (NSERC) Discovery Program. Sequences were deposited in GenBank, accession numbers EF434458 to EF434504.

Supporting Online Material

www.sciencemag.org/cgi/content/full/315/5819/1709/DC1
Materials and Methods
Figs. S1 to S5
References and Notes

29 November 2006; accepted 16 February 2007
10.1126/science.1138140

A G Protein–Coupled Receptor Is a Plasma Membrane Receptor for the Plant Hormone Abscisic Acid

Xigang Liu,^{1,2} Yanling Yue,¹ Bin Li,³ Yanli Nie,¹ Wei Li,² Wei-Hua Wu,³ Ligeng Ma^{1,2*}

The plant hormone abscisic acid (ABA) regulates many physiological and developmental processes in plants. The mechanism of ABA perception at the cell surface is not understood. Here, we report that a G protein–coupled receptor genetically and physically interacts with the G protein α subunit GPA1 to mediate all known ABA responses in *Arabidopsis*. Overexpressing this receptor results in an ABA-hypersensitive phenotype. This receptor binds ABA with high affinity at physiological concentration with expected kinetics and stereospecificity. The binding of ABA to the receptor leads to the dissociation of the receptor-GPA1 complex in yeast. Our results demonstrate that this G protein–coupled receptor is a plasma membrane ABA receptor.

Abscisic acid (ABA) is an important hormone that mediates many aspects of plant growth and development, particularly in response to the environmental stresses (1–3). Several components involved in the ABA signaling pathway have been identified (4). Two recent reports have shown that the nuclear RNA binding protein flowering time control protein (FCA) (5) and the chloroplast protein Mg chelatase H subunit (6) are ABA receptors (6).

In contrast, several earlier experiments had suggested that extracellular perception is critical for ABA to achieve its functions (7–9). Thus, other ABA receptors, especially plasma membrane–localized receptors, may be the major players for perceiving extracellular ABA and mediating the classic ABA signaling responses.

Ligand-mediated signaling through G protein–coupled receptors (GPCRs) is a conserved mechanism for the extracellular signal perception at the plasma membrane in eukaryotic organisms (10). The GPCR-mediated signaling pathway plays a central role in vital processes such as vision, taste, and olfaction in animals (11). However, the higher plant *Arabidopsis thaliana* has only one canonical $G\alpha$ (GPA1) subunit, one $G\beta$ subunit, and two $G\gamma$ subunits (12–16). The significance of these subunits in plant systems is poorly understood; only one

Arabidopsis putative GPCR protein (GCR1) has been characterized in plants (17–20), and no ligand has been defined for any plant GPCR.

To identify previously unrecognized GPCR proteins in *Arabidopsis*, we started by searching the *Arabidopsis* genome and found a gene (*GCR2*, GenBank accession code At1g52920) encoding a putative GPCR. Transmembrane structure prediction suggests that GCR2 is a membrane protein with seven transmembrane helices (fig. S1, A and B). The subsequent cellular localization analysis confirmed its plasma membrane localization in the transgenic plant root (fig. S1C). GCR2–yellow fluorescent protein (YFP) is detected in the membrane fraction isolated from the GCR2-YFP transgenic plant. Similar to GCR1 (19), GCR2 is mostly associated with the membrane fraction (fig. S1D). Furthermore, even after washing with detergent or a higher pH buffer, GCR2 is retained with the membrane fraction, suggesting that GCR2 is an integral membrane protein (fig. S1D).

One feature of the GPCR is its ability to interact with G protein to form a complex. To confirm the physical interaction between GCR2 and $G\alpha$, we used four different approaches to detect their interaction. We first used surface plasmon resonance spectroscopy to investigate the interaction between GCR2 and GPA1. For this purpose, we expressed and purified recombinant GCR2 and GPA1 proteins in bacteria (fig. S2). This in vitro assay clearly indicated that GPA1 is capable of binding to GCR2, whereas no binding activity was detected between GPA1 and bovine serum albumin (BSA) (fig. S3, A and B). The dissociation binding constant (K_d) for GCR2 and GPA1 is 2.1×10^{-9} M (fig. S3C).

¹National Institute of Biological Sciences, 7 Science Park Road, Zhongguancun Life Science Park, Beijing 102206, China.

²Laboratory of Molecular and Cellular Biology, Hebei Normal University, Shijiazhuang, Hebei 050016, China. ³State Key Laboratory of Plant Physiology and Biochemistry, College of Biological Sciences, China Agricultural University, Beijing 100094, China.

*To whom correspondence should be addressed. E-mail: maligeng@nibs.ac.cn